Radiocarbon, Vol 60, Nr 1, 2018, p 21–34 DOI:10.1017/RDC.2017.100

CHANGES IN CO_2 EMISSION SOURCES IN MEXICO CITY METROPOLITAN AREA DEDUCED FROM RADIOCARBON CONCENTRATIONS IN TREE RINGS

Laura E Beramendi-Orosco[1,3*] • Galia González-Hernández[2,3] • Angeles Martínez-Reyes[4] • Ofelia Morton-Bermea[2] • Francisco J Santos-Arévalo[5] • Isabel Gómez-Martínez[5] • José Villanueva-Díaz[6]

[1]Instituto de Geología, Universidad Nacional Autónoma de México, Ciudad Universitaria, 04510, México.
[2]Instituto de Geofísica, Universidad Nacional Autónoma de México, Ciudad Universitaria, 04510, México.
[3]Laboratorio Universitario de Radiocarbono, Laboratorio Nacional de Geoquímica y Mineralogía, Ciudad Universitaria, 04510, México.
[4]Posgrado en Ciencias Biológicas, Universidad Nacional Autónoma de México, Ciudad Universitaria, 04510, México.
[5]Centro Nacional de Aceleradores (Universidad de Sevilla, CSIC, Junta de Andalucía), Avda. Thomas Alva Edison 7, Isla de la Cartuja, Seville, 41092, Spain.
[6]Laboratorio Nacional de Dendrocronología, Instituto Nacional de Investigaciones Forestales Agrícolas y Pecuarias, Gómez Palacio, Durango, Apdo. Postal 41, México.

ABSTRACT. We present radiocarbon (^{14}C) in tree rings from Mexico City and a reconstruction of fossil CO_2 concentrations for the last five decades, as part of a research program to understand the ^{14}C dynamics in this complex urban area. Background values were established by ^{14}C concentrations in tree rings from a nearby clean area. Agreement between background and NH-zone 2 values indicate *Taxodium mucronatum* is a good biomonitor for annual atmospheric ^{14}C variations. Values for the urban tree rings were significantly lower than background values, indicating a ^{14}C depletion from fossil CO_2 emissions. There is an increasing trend of fossil CO_2 between 1960 and 1990, in agreement with the population growth and the increasing demand for fossil fuels in Mexico City. Between 1990 and 2000, there is an apparent decrease in fossil CO_2 concentration, increasing again after 2000. The decrease in 2000, despite being of the same magnitude as the overall uncertainty, may reflect environmental policies that improved the energy efficiency and reduced CO_2 emissions in the area. The increase in fossil CO_2 concentration between 2000 and 2010 may be attributable to the significant growth of motor vehicle usage in Mexico City, which made transportation the main energy-demanding and -emitting sector.

KEYWORDS: emission sources, fossil CO_2, Mexico City, tree rings.

INTRODUCTION

Radiocarbon (^{14}C) can be used as a tracer for fossil-fuel-derived CO_2 to estimate anthropogenic emissions because fossil fuels are ^{14}C-free as a result of their age of several million years. The increase in the use of fossil fuels to cover the energy demand has altered the carbon isotopic composition of atmospheric CO_2 especially in urban areas, making it possible to estimate the fossil CO_2 contribution by an isotopic mass balance, comparing the ^{14}C concentration in atmospheric CO_2 ($^{14}CO_2$) in an urban area with the concentration of $^{14}CO_2$ in "clean" air from areas isolated from anthropogenic CO_2 sources (Levin et al. 2003; Turnbull et al. 2006). This can be achieved either by monitoring the $^{14}CO_2$ in the urban and clean atmospheres (Levin et al. 2003; Graven et al. 2009) or by analyzing the ^{14}C concentrations found in annual plants (Hsueh et al. 2007) or tree rings (Rakowski et al. 2008; Capano et al. 2010; Djuricin et al. 2012). Further, it has been demonstrated that tree rings are good biomonitors of the ^{14}C concentration of atmospheric CO_2 with annual, or even sub-annual, time resolution (Grootes et al. 1989; Hua and Barbetti 2004).

The Mexico City Metropolitan Area (MCMA) is a complex urban area with more than 21 million inhabitants located in a high-altitude (~2300 m asl) closed basin covering an area of 7800 km^2. Considered the biggest megacity in North America, it produces high volumes of gases and aerosols derived from a variety of emission sources, including more than 5.9 million vehicles, 30,000 industries, 5.8 million households, 3 landfills, and around 900 km^2 of rural,

*Corresponding author. Email: laurab@geologia.unam.mx.

forest, and shrub-land soils (SEDEMA 2016). The rapid population growth that began in the 1950s (Escamilla-Herrera and Santos-Cerquera 2012) resulted in a significant deterioration of the environment, which is reflected in poor air quality. The frequency of extremely high pollution events during the last years of the 1980s encouraged the implementation of a series of environmental policies through the PICCA (Primer Programa Integral contra la Contaminación Atmosférica) and PROAIRE (Programa para Mejorar la Calidad del Aire en el Valle de México) programs (DDF 1990, 1996).

Some of the environmental strategies included the decentralization of the industrial sector, the closure in 1991 of a refinery with capacity of 7500 barrels of petroleum per day, emission controls for industry, introduction of catalytic converters in motor vehicles and the addition of oxygenated compounds to gasoline to improve the combustion efficiency and reduce contaminants, as well as circulation restriction once a week for private motor vehicles, among others (DDF 1990, 1996). With the introduction of these environmental programs, the number of days with air quality worse than the local standards reduced significantly, improving energy efficiency and reducing CO_2 emissions during the 1990s (SEDEMA 2012). However, the MCMA continued its unplanned growth during the first decade of the 21st century, further deteriorating the environment despite the programs implemented in the 1990s. It becomes relevant not only to continue the pollution monitoring programs and produce emission inventories, but also to try to reconstruct the CO_2 emissions history to evaluate the effect of the environmental policies.

The few previous studies of atmospheric $^{14}CO_2$ in the MCMA have reported anomalously high ^{14}C levels. Vay et al. (2009) reported $\Delta^{14}C$ values of up to 75‰ higher than the background for CO_2 samples collected in MCMA during March 2006. They attributed this to an important contribution from ^{14}C-enriched CO_2 sources, such as burning of biomass with a mean age of 35 yr and $\Delta^{14}C$ of around 500‰, or even other hotter sources including burning of radioactive wastes from hospitals and $^{14}CO_2$ emitted by the Laguna Verde nuclear power plant on the Gulf of Mexico coast, 290 km from MCMA. Further, a study of spatial variations of $^{14}CO_2$ in integrated atmospheric CO_2 samples also reported values higher than background for samples taken during the dry-warm season. This was attributed to emissions of ^{14}C-enriched CO_2 during the frequent forest fires in the mountains during the sampling period (Beramendi-Orosco et al. 2015). Initial results for tree rings were reported in the same work, with an apparent higher ^{14}C-dilution during the 1960s than in the recent years, despite the population increase and thus the growth in the consumption of fossil fuels since the 1970s. From these works it becomes evident that the ^{14}C dynamics in such a complex city makes the direct use of ^{14}C as a tracer fossil CO_2 a difficult task that deserves attention.

This work is part of a research program that aims to understand the ^{14}C dynamics in the MCMA and identify CO_2 emission sources, and eventually contribute to validation of the emissions inventories. Here we report ^{14}C concentrations in tree rings from an urban forest within the MCMA and a reconstruction of the fossil CO_2 concentration for the last five decades.

MATERIALS AND METHODS

Sampling Sites

The sampling site within the MCMA was Bosque de Chapultepec, the largest public park in the city. It is an urban forest located within the downtown district in the northwest area of Mexico City (from 19°23′40″ to 19°25′45″N and 99°10′40″ to 99°14′15″W, Figure 1). The vegetation includes 130 native and introduced species, with ahuehuete or sabino (*Taxodium mucronatum* Ten.) as one

https://doi.org/10.1017/RDC.2017.100 Published online by Cambridge University Press

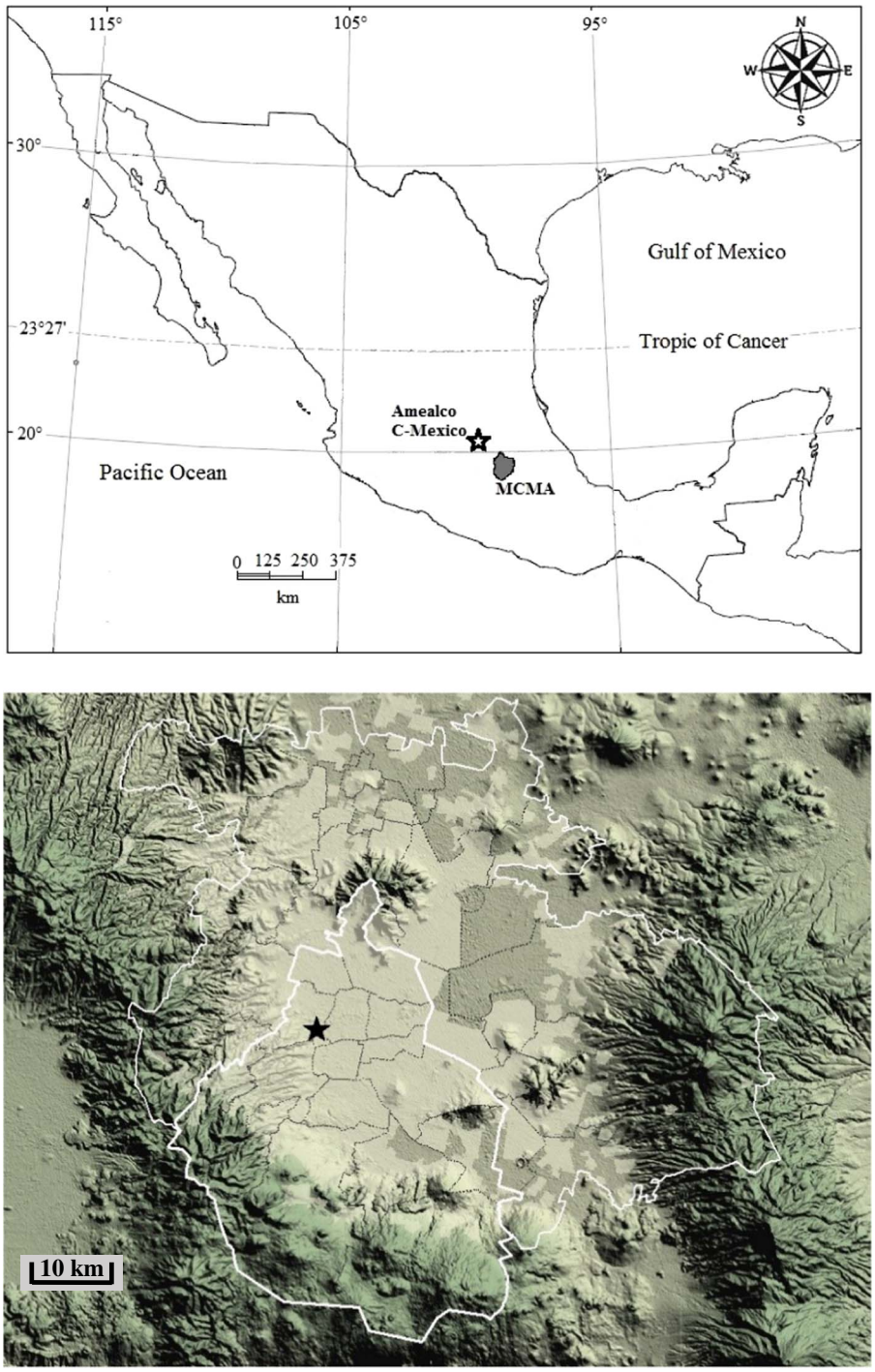

Figure 1 (Top) Map of Mexico showing location of Mexico City Metropolitan Area (grey area) and the background site in central Mexico (black star); (bottom) relief map of the MCMA showing sampling site (black star) and the limits of Mexico City and the Metropolitan Area (white lines). Maps modified from INEGI (2016) (http://cuentame.inegi.org.mx/mapas/nacional.aspx?tema = M).

https://doi.org/10.1017/RDC.2017.100 Published online by Cambridge University Press

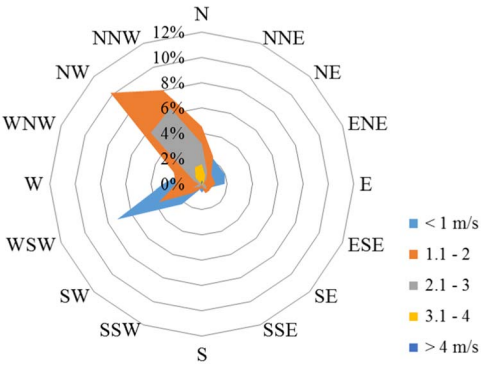

Figure 2 Wind rose for the sampling area in MCMA for 2010 (data correspond to Tacuba meteorological station, located 4 km to the NNW of Chapultepec Park, available from http://www.aire.cdmx.gob.mx/default.php?opc=%27aKBhnmI=%27&opcion=Zw==).

of the dominant native tree species. This sampling site was selected based on the fact that this location has been inside the urban area for centuries, and because it opens the possibility of sampling trees that are exposed to a more representative atmosphere of the city and not directly exposed to a main emission source, as would be trees growing adjacent to main avenues. Further, a master *T mucronatum* Ten. dendrochronology has been previously reported for this site (Villanueva-Diaz et al. 2003). The climate in MCMA is tempered by altitude and influenced by tropical air masses during summer (May to October) and mid-latitude cold air masses from North America during winter (Jauregui 2004). The mean annual temperature is 16°C and the annual precipitation, concentrated during the summer months, is 700–1200 mm in the central and southern parts (Jauregui 2004; INEGI 2014). The dominant wind direction in the sampling area is from the NW (Figure 2).

The sampling site selected as a background area representative for latitudes close to Mexico City corresponds to Barranca de Amealco, Querétaro (20°21′50″N, 100°06′22″W, Figure 1), a steep gorge located in an uncontaminated area away from the influence of urban areas, 140 km from Mexico City. This site was selected because the same tree species is present and a master tree-ring chronology has already been reported (Stahle et al. 2011).

Tree-Ring Sampling and Dendrochronological Dating

Healthy and relatively young specimens of *T mucronatum* Ten., the dominant native species present at both sampling sites, were sampled using a 12-mm Pressler incremental borer at about 1.5 m height, taking three increment cores from each tree to assure an accurate dating and avoid false or missing rings. Trees were selected based on the diameter at breast height to have a similar age and to cover a time period back to at least 1950. Sampling in the Bosque de Chapultepec site was performed in May 2012 and in Barranca de Amealco during March 2013.

Samples were mounted on wooded core mounts, dried for 48 hr at 60°C, and sanded with increasing grit number sandpaper (400–1500) to expose cell structures (Stokes and Smiley 1968). To avoid cross-ring contamination, the generated dust was removed with a brush and vacuum. The annual rings were counted under stereoscopic microscopes and the chronologies

https://doi.org/10.1017/RDC.2017.100 Published online by Cambridge University Press

were established by comparison with the master chronologies already reported for this species (Villanueva-Diaz et al. 2003; Stahle et al. 2011).

Sample Preparation and Analysis

Rings exactly dated to their years of formation, from a single tree from each sampling site, were separated using a stainless steel blade and cut into small pieces to facilitate the pretreatment procedure. Sample pretreatment and accelerator mass spectrometry (AMS) analyses were performed at the Centro Nacional de Aceleradores, Seville, Spain. Samples were cleaned by Soxhlet extraction using a solvent sequence of hexane, acetone, and ethanol, followed by cellulose extraction applying the procedure reported in Nemec et al. (2010). Prior to analysis, samples were graphitized using an automated graphitization equipment (AGE) system (Wacker et al. 2010a), which couples an elemental analyzer to the graphitization unit. Approximately 3 mg of clean and dry cellulose was combusted in an elemental analyzer using tin foils to wrap the sample. The gases produced during the combustion are released sequentially as the temperature in a chromatographic column increases. When CO_2 is released, the gas is injected into the corresponding reactor in the graphitization unit, containing Fe as a catalyst. Finally, H_2 is added to the reactor. Once all the reactors have been filled, the reaction takes place. Ovens heat the lower part of the reactor where the CO_2 is reduced to graphite and adheres to the iron, and Peltier coolers are used to freeze the water produced in the reaction. The system prepares samples of ca. 1 mg C.

Analyses were performed using the MICADAS system (Synal et al. 2007). The MICADAS uses a 200 kV power supply to accelerate ions to the stripper, selecting charge state 1+ after the stripping process, for a total ion energy of 440 keV. ^{14}C ions are counted in an ionization chamber, and stable isotopes are measured in corresponding Faraday cups at the high energy side. The major interference in the identification of ^{14}C is the scattered molecular fragment ^{13}C coming from the ^{13}CH molecule, which cannot be identified by the signal in the ionization chamber. Thus, a special Faraday cup located next to the others measures the current from this molecular fragment, allowing a correction in the number of counts given by the detector. Samples were measured for 1 hr and data were analyzed using the BATS tool software (Wacker et al. 2010b). Oxalic acid II (SRM 4990C) was used as the normalization standard. The ^{14}C results are reported as $F^{14}C$ and $\Delta^{14}C$ corrected for both isotopic fractionation and decay (Stuiver and Polach 1977; Reimer et al. 2004).

Fossil CO_2 Calculations

The rationale for estimating the concentration of fossil CO_2 ($[CO_2]_{fossil}$) through an isotopic mass balance has been reported previously by other research groups (see for example Levin et al. 2003, 2008; Turnbull et al. 2006, 2016). The concentration of fossil CO_2 was estimated using Equation 1, considering that fossil fuels do not contain ^{14}C ($F^{14}C = 0$).

$$[CO_2]_{fossil} = [CO_2]_{Bkg}\left(\frac{F^{14}C_{Bkg} - F^{14}C_{sample}}{F^{14}C_{Bkg}}\right) + [CO_2]_{Other}\left(\frac{F^{14}C_{Other} - F^{14}C_{Bkg}}{F^{14}C_{Bkg}}\right) \quad (1)$$

where $[CO_2]_{fossil}$ is the estimated mole fraction, in ppm, of CO_2 derived from fossil emissions sources, $[CO_2]_{Bkg}$ is the atmospheric CO_2 mole fraction in the background area, $F^{14}C_{Bkg}$ and $F^{14}C_{sample}$ are the ^{14}C concentrations in tree rings from the background and the MCMA sampling sites, respectively. The second term of the equation corresponds to the CO_2 contributions from non-fossil sources, including heterotrophic respiration, biomass burning and emissions from nuclear industry (i.e. nuclear power plants and combustion of radioactive medical wastes),

https://doi.org/10.1017/RDC.2017.100 Published online by Cambridge University Press

among others, where $[CO_2]_{Other}$ is the mole fraction of this non-fossil CO_2 in the local atmosphere and $F^{14}C_{Other}$ is the weighted mean radiocarbon concentration in these sources (Turnbull et al. 2016). Despite that the contribution from this term to the calculated $[CO_2]_{fossil}$ is usually small, especially in urban areas, it should be accounted for (Turnbull et al. 2006; Levin et al. 2008). In the MCMA, the main non-fossil CO_2 sources are heterotrophic respiration and biomass burning, with a negligible contribution from nuclear industry. The heterotrophic respiration and biomass burning can have similar $F^{14}C$, as both derive from organic matter with a mean age of the same order, and their contribution to the $[CO_2]$ mole fraction can be variable, with heterotrophic respiration being larger during the raining summer months and biomass burning during the dry season (winter–early spring) either from forest fires and/or from biomass combustion as fuel. Because the period when the tree fixes most of the carbon in the growth-rings is the summer, we consider heterotrophic respiration as the main factor in this term. Regarding the nuclear industry sources, we consider this is smaller than the overall uncertainty of the $[CO_2]_{fossil}$ because the only nuclear power plant in Mexico (Laguna Verde, Veracruz on the Gulf of Mexico coast) is located 300 km to the E of the MCMA, and it has been reported that the effect from these sources to the estimated $[CO_2]_{fossil}$ is of the order of −0.25 ppm over large regions, becoming significant (higher than the overall uncertainty) only in the vicinity of nuclear sites (Graven and Gruber, 2011). With these considerations, we estimated $[CO_2]_{Other}$ to be 5 ppm, which corresponds to the value proposed by Turnbull et al. (2006) for summer and $F^{14}C_{Other}$ was calculated assuming a terrestrial carbon mean residence time of 10 yr. With these assumptions, the magnitude of this term ranges between –1 and 0.4 ppm, with values for the 1960–1980 period being negative because the organic matter was ^{14}C-depleted as compared to the atmosphere, indicating that not considering respiration would result in overestimating the calculated $[CO_2]_{fossil}$, whereas the positive values obtained for the las decades indicate that if not considered, the fossil CO_2 mole fraction would be sub-estimated because for the post-1980 the heterotrophic respiration became a ^{14}C source to the atmosphere (Randerson et al. 2002). However, the magnitude of this contribution is smaller than the overall uncertainty of $[CO_2]_{fossil}$.

The overall uncertainty of the calculated $[CO_2]_{fossil}$ was estimated by considering the combination of component errors according to the following model (Doebelin 1990):

$$\Delta[CO_2]_{fossil} = \left|\Delta u_1 \frac{\partial[CO_2]_{fossil}}{\partial u_1}\right| + \left|\Delta u_2 \frac{\partial[CO_2]_{fossil}}{\partial u_2}\right| + \left|\Delta u_3 \frac{\partial[CO_2]_{fossil}}{\partial u_3}\right| + \left|\Delta u_4 \frac{\partial[CO_2]_{fossil}}{\partial u_4}\right| \quad (2)$$

where Δ denotes uncertainty, u_1 corresponds to $[CO_2]_{Bkg}$, u_2 to $F^{14}C_{Bkg}$, u_3 to $F^{14}C_{sample}$, and u_4 to $F^{14}C_{Other}$. The terms with strongest influence on the overall error are $F^{14}C_{Bkg}$ and $F^{14}C_{sample}$, resulting in uncertainties higher than ± 2.5 ppm.

Finally, the $[CO_2]_{Bkg}$ has not been measured in the background sampling area, so we assume this corresponds to the annual mean values reported for Mauna Loa monitoring station, considered as representative of global clean air (Tans and Keeling 2016).

RESULTS AND DISCUSSION

Radiocarbon concentrations in tree rings from both sampling sites are plotted in Figure 3 and tabulated in Table 1. Tree ring ^{14}C data from the Northern Hemisphere zone 2 curve (NH-2) compiled by Hua et al. (2013) are plotted for comparison and assessment of the results obtained.

https://doi.org/10.1017/RDC.2017.100 Published online by Cambridge University Press

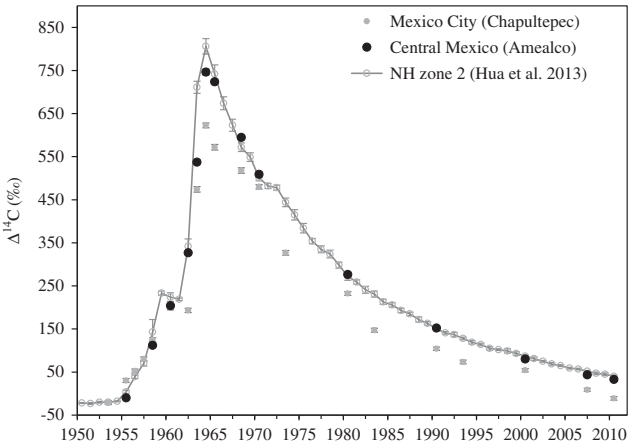

Figure 3 $\Delta^{14}C$ values for tree rings from Chapultepec Park, Mexico City (grey circles), and tree rings from Amealco (Central Mexico background, black circles). Background values from NH zone 2 (Hua et al. 2013, line with open circles) are plotted for comparison. Vertical error bars correspond to $\pm 1\sigma$, but for most of the samples symbols are bigger than the error.

Establishing Background Atmospheric ^{14}C Concentrations for Central Mexico—^{14}C Variations in Amealco

The results obtained for Amealco (C-Mexico) tree rings are in good agreement with the NH-2 curve (Figures 3 and 4), with a highly significant correlation coefficient ($r = 0.987$, $P < 0.001$) and the bomb peak centered during 1964. These results demonstrate the annual nature of *T mucronatum* growth rings and indicate that the dendrochronological dating was accurate. However, there are significant differences in the magnitude of the ^{14}C excess during the sharp increase of the bomb peak years (1963 and 1964, Table 2), with values for the Amealco tree rings significantly lower than the NH-2 curve by 174 and 60‰, respectively. These differences may be a consequence of atmospheric circulation in Central Mexico, characterized by winds from the south, carrying ^{14}C-depleted air during the summer months (Beramendi-Orosco et al. 2010). Values for post-1970 years are in close agreement with the NH values, as a consequence of the global distribution of excess ^{14}C; however, because the NH-zone 2 values do not include ^{14}C data from North America and the compilation considered only datasets that were not strongly influenced by regional fossil CO_2 emissions (a dilution within the $\pm 1\sigma$ of analytical uncertainty; Hua et al. 2013), the selection of the background dataset is a relevant issue in order to make a better estimate of the local radiocarbon dilution (Turnbull et al. 2015). The C-Mexico ^{14}C values for 1970, 1980, and 1990 tree rings are within $\pm 1\sigma$ of the Hua et al. (2013) compilation, but values for 2000, 2007, and 2010 tree rings, despite being within $\pm 2\sigma$, C-Mexico values are lower than the mean values for the NH hemisphere (Table 2), reflecting some dilution as a result of regional fossil CO_2 emissions over Central Mexico. Because our aim is to estimate the local $[CO_2]_{fossil}$ for the central area of the MCMA, using NH-zone 2 data as background would result in overestimating the radiocarbon dilution, as it would consider the local emissions the tree is exposed to but also the regional fossil emissions (Turnbull et al. 2015). With this consideration, the Amealco tree ring ^{14}C data would seem a more appropriate regional background for Central Mexico, and was further evaluated by HYSPLIT model back trajectories (Stein et al. 2015; Rolph et al. 2017) for the beginning and end of the growing season (March and September) for years 1990, 2000, and 2010, confirming that this dataset is indeed

https://doi.org/10.1017/RDC.2017.100 Published online by Cambridge University Press

Table 1 Radiocarbon values for *Taxodium mucronatum* Ten. tree-ring samples from Chapultepec Park (Mexico City) and from Amealco, Querétaro (Central Mexico, background site).

Sample code (CNA-)	Year (AD)	$F^{14}C \pm 1\sigma$	$\Delta^{14}C \pm 1\sigma$ (‰)
Chapultepec Park, Mexico City			
2647.1.1	1953.5	0.9793 ± 0.0044	–21.1 ± 4.4
2645.1.1	1955.5	1.0311 ± 0.0046	30.4 ± 4.6
2644.1.1	1956.5	1.0531 ± 0.0047	52.3 ± 4.7
2646.1.1	1957.5	1.0813 ± 0.0048	80.3 ± 4.8
2814.1.1	1958.5	1.1258 ± 0.0047	124.7 ± 4.7
2643.1.1	1960.5	1.2011 ± 0.0052	199.6 ± 5.2
2813.1.1	1962.5	1.1949 ± 0.0049	193.1 ± 4.9
2642.1.1	1963.5	1.4765 ± 0.0064	474.1 ± 6.4
3688.1.1	1964.5	1.6254 ± 0.0055	622.5 ± 5.5
2815.1.1	1965.5	1.5749 ± 0.0064	571.9 ± 6.4
2816.1.1	1968.5	1.5213 ± 0.0062	517.9 ± 6.2
3689.1.1	1970.5	1.4838 ± 0.0051	480.1 ± 5.1
2641.1.1	1973.5	1.3306 ± 0.0053	326.8 ± 5.3
3690.1.1	1980.5	1.2369 ± 0.0043	232.3 ± 4.3
2640.1.1	1983.5	1.1518 ± 0.0046	147.1 ± 4.6
3691.1.1	1990.5	1.1096 ± 0.0039	104.2 ± 3.9
2638.1.1	1993.5	1.0791 ± 0.0043	73.4 ± 4.3
3692.1.1	2000.5	1.0606 ± 0.0038	54.2 ± 3.8
3693.1.1	2007.5	1.0159 ± 0.0036	8.9 ± 3.6
2638.1.1	2010.5	0.9962 ± 0.0041	–11.1 ± 4.1
Amealco, Central Mexico			
3682.1.1	1955.5	0.9909 ± 0.0036	9.8 ± 3.6
3683.1.1	1958.5	1.1135 ± 0.0039	112.3 ± 3.9
2637.2.1	1960.5	1.2056 ± 0.0052	204.0 ± 5.2
3684.1.1	1962.5	1.3287 ± 0.0045	326.7 ± 4.5
3685.1.1	1963.5	1.5399 ± 0.0052	537.4 ± 5.2
2636.2.1	1964.5	1.7495 ± 0.0071	746.4 ± 7.1
3686.1.1	1965.5	1.7272 ± 0.0063	724.0 ± 6.3
3687.1.1	1968.5	1.5982 ± 0.0054	594.6 ± 5.4
2635.2.1	1970.5	1.5128 ± 0.0063	509.0 ± 6.3
2634.2.1	1980.5	1.2811 ± 0.0055	276.4 ± 5.5
2633.2.1	1990.5	1.1581 ± 0.0050	152.5 ± 5.0
2632.2.1	2000.5	1.0868 ± 0.0048	80.2 ± 4.8
2631.2.1	2007.5	1.0509 ± 0.0046	43.6 ± 4.6
3936.1.1	2010.5	1.0406 ± 0.0036	33.0 ± 3.6

appropriate as background for the MCMA as both sites receive air mases from similar regions (Figure 5).

Temporal Variations of ^{14}C in Tree Rings from the Mexico City Metropolitan Area

An important feature of the Mexico City record is that the bomb-peak is centered during 1964, confirming the accurate dating of the annual growth bands of *T. mucronatum*. The $\Delta^{14}C$ values are lower than values from both background records (C-Mexico and NH-2), except for the 1955–1957 period. Although the ^{14}C depletion in the Mexico City record was expected as it is an

https://doi.org/10.1017/RDC.2017.100 Published online by Cambridge University Press

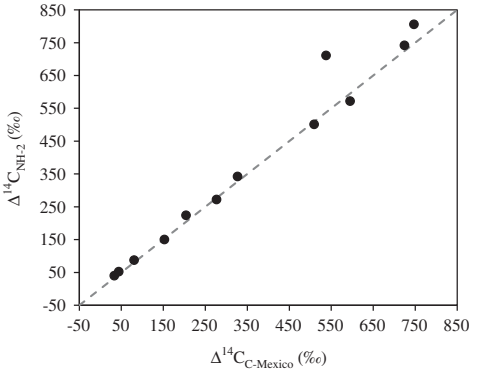

Figure 4 $\Delta^{14}C$ values for Central Mexico tree rings versus NH zone 2 values. The dashed line represents the line of identity.

Table 2 Difference between $\Delta^{14}C$ values obtained for Amealco, Central Mexico, and data from the NH-zone 2 curve (Hua et al. 2013). Significant differences are marked in bold.

Year (AD)	Central Mexico NH zone 2	±1σ Central Mexico	±1σ NH zone 2
1960.5	–20	5.2	1
1962.5	–15	4.5	17
1963.5	**–174**	5.2	14
1964.5	**–60**	7.1	18
1965.5	–18	6.3	21
1970.5	8	6.3	7
1980.5	4	5.5	9
1990.5	2	5.0	5
2000.5	–7	4.8	3
2007.5	–8	4.6	2
2010.5	–7	3.6	3

urban area with vast volume of fossil-fuel-derived CO_2 emissions; it appears that the ^{14}C dilution is not constant. During the 1960s the $\Delta^{14}C$ values are up to 134‰ lower than the C-Mexico values, whereas for the 1970–2010 period the values for the Mexico City tree rings are between 26 and 49‰ lower than the background values. A possible explanation for the high ^{14}C dilution found for the 1960s may be related to different factors such as the heterogeneity of the excess $^{14}CO_2$ during those years and the geography of the Mexico City Basin, and not to a higher volume of fossil CO_2 emissions, which was not a dominant factor of the $\Delta^{14}C$ spatial variability during the years of the sharp increase of atmospheric radiocarbon (Turnbull et al. 2016). Furthermore, during the first years of the ^{14}C perturbation, heterotrophic respiration was relatively depleted in ^{14}C as compared to the local atmosphere, because it derived from pre-bomb organic matter, and became relatively enriched during the 1980s as it derived from organic matter that had assimilated the bomb ^{14}C (Randerson et al. 2002). This may also explain the higher ^{14}C dilution during the peak years (1962–1967) that have been reported for tree rings from other urban areas (Rakowski et al. 2001, 2008; Beramendi-Orosco et al. 2013).

https://doi.org/10.1017/RDC.2017.100 Published online by Cambridge University Press

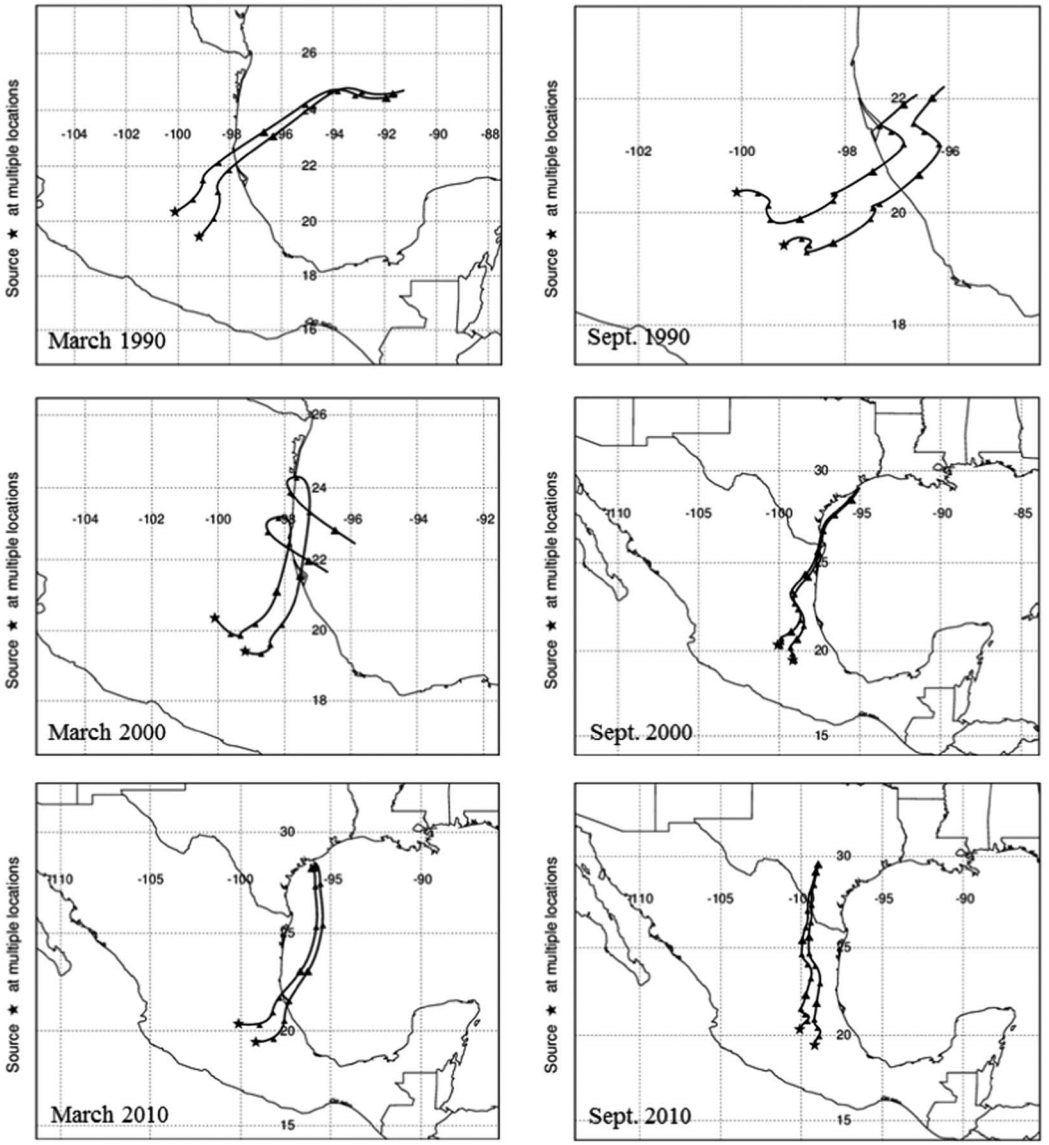

Figure 5 Three-day air back-trajectories for the beginning and ending of the growing season at MCMA and Central Mexico produced by HYSPLIT (Stein et al. 2015; Rolph et al. 2017) at 10 m above ground level using the REANALYSIS dataset.

Fossil CO_2 Concentration and Possible CO_2 Emission Sources in MCMA

The reconstruction of the fossil CO_2 concentration was evaluated excluding the bomb-peak years in order to avoid the years with high atmospheric ^{14}C heterogeneity (Figure 6). As discussed above, the $[CO_2]_{fossil}$ were calculated using C-Mexico data as background to estimate the local contribution of fossil CO_2. The obtained values range between 5.5 and 16.5 ppm (overall uncertainties range between ±2.9 and ±3.2), with a general increasing trend; however, a fossil-CO_2 decrease between 1990 and 2000 is apparent with a further increase between 2000 and 2010. The increase in fossil CO_2 mole fraction since 1960 was expected, as the population

https://doi.org/10.1017/RDC.2017.100 Published online by Cambridge University Press

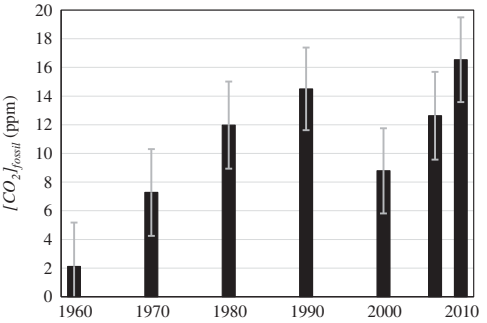

Figure 6 Reconstruction of the fossil CO_2 mole fraction (in parts per million, ppm) in Mexico City using Central Mexico (C-Mexico) $\Delta^{14}C$ values as background. Error bars represent the overall uncertainty and range between 2.9 and 3.2 ppm.

grew from 9 million inhabitants to 14.9 million in 1990, and to more than 20 million in 2010 (Escamilla-Herrera and Santos-Cerquera 2012). The population growth increased the energy demand and thus fossil fuels consumption, as well as CO_2 emission sources containing ^{14}C, such as biomass burning, either as a fuel or in fires intentionally set to clear land for the expanding urban area, and heterotrophic respiration. Biomass burning, however, is assumed to have a not significant effect in the tree ring $\Delta^{14}C$ values, as they integrate mainly carbon fixed during the summer months, when this is not a significant source of CO_2. By contrast, heterotrophic respiration may have increased as a result of deforestation for expanding the urban area because the effect of such disturbance may result in transforming the ecosystem from a C sink to a CO_2 source to the atmosphere (Harmon et al. 2011), thus could have an effect during the summer months; however, the contribution from this source to the estimated $[CO_2]_{fossil}$ is smaller than the overall uncertainty.

Notwithstanding the tree ring $\Delta^{14}C$ values and the corresponding estimated $[CO_2]_{fossil}$ reflect only the local CO_2 the tree is assimilating, the fact that the sampling site is located in the downtown district enables us to consider these values as representative of the central urban area. The apparent decrease in $[CO_2]_{fossil}$ between 1990 and 2000, although being of the same magnitude as the associated uncertainty, may reflect the implementation of the environmental policy programs implemented during the 1990s (PICCA in 1991 and PROAIRE in 1996), even though total fossil fuel consumption in the MCMA increased from 34,632 thousand barrels/year in 1990 to 43,365 thousand barrels/year in 2000, mainly as a result of the population increase in peripheral urban areas (SEDEMA 2000). Among the measures that may have had an effect in the local fossil CO_2 mole fraction are the closure of the refinery in 1991 and the mandatory one-day per week no-circulation program, which reduced by 20% the number of private vehicles circulating in the area every weekday. The refinery was located 5 km NNW from the tree-ring sampling site, downwind in the path of the dominant wind direction (Figure 2), so it was presumably a significant fossil CO_2 source in the tree sampling area. In contrast, from 2000 to 2010 the carbon economy intensified, resulting in a significant increase in motor vehicle usage, doubling the number of registered private vehicles between 2000 and 2010 and increasing the time spent in road traffic, especially in the central urban area (OECD 2013). This made transportation the main energy-demanding and polluting sector in the last decade, despite the cleaner technologies and fuels implemented during the 1990s (SEDEMA 2012).

https://doi.org/10.1017/RDC.2017.100 Published online by Cambridge University Press

These changes seem to be reflected in the $F^{14}C$ of tree rings and the estimated fossil CO_2 mole fraction, which nearly doubled in the 2000s decade.

Variability of atmospheric transport may be another factor having influence on the variations of estimated $[CO_2]_{fossil}$, changing the contribution from the different CO_2 sources available to the tree (Levin and Rödenbeck 2008; Keller at al. 2016). However, the fact that the sampling site is an urban forest immersed in the city and surrounded by important avenues, making traffic the main CO_2 source, suggests that changes in the wind direction would have a small impact on the variations we are finding.

Finally, as mentioned in the introduction, previous studies have found higher than background $F^{14}C$ values for instantaneous and monthly integrated atmospheric CO_2 samples from the MCMA during the dry warm season (March–April), suggesting considerable CO_2 emissions from ^{14}C-enriched sources, such as burning of biomass and topsoil organic matter during forest fires (Vay et al. 2009; Beramendi-Orosco et al. 2015). However, the contribution from these ^{14}C-enriched CO_2 sources to the tree rings $\Delta^{14}C$ values and the $[CO_2]_{fossil}$ estimated here seems to be not significant because the tree rings integrate the local CO_2 assimilated mainly during the wet summer months, when these sources are smaller because forest fires are not common.

CONCLUSIONS

The $F^{14}C$ values obtained indicate that tree rings of *Taxodium mucronatum* Ten. are good biomonitors of the atmospheric $^{14}CO_2$ concentration with annual resolution, allowing not only the reconstruction of the ^{14}C bomb-peak variation for C-cycle studies, but also the estimation of fossil CO_2 concentration in urban areas. This is relevant because this tree species is widely distributed in North America, particularly in Mexico, where there has been a lack of information on the $^{14}CO_2$ concentration throughout the 20th century.

Establishing background atmospheric ^{14}C concentrations for Central Mexico is important because the NH-2 curve does not include data from North America, and previous studies had reported that the ^{14}C bomb-peak variation for NW Mexico was significantly lower than the NH-2 values. Further, having a background representative for Central Mexico enables a more accurate estimation of the local fossil CO_2 concentration in Mexico City.

The reconstruction of the fossil CO_2 concentration for Mexico City suggests there was a positive impact of the implementation of environmental programs in the 1990s, but highlights the worrying increase since 2000, this presumably as a result of the increase in motor vehicle usage in the MCMA. More work is needed to gain a better understanding of the factors that influence the $[CO_2]_{fossil}$ variations we are finding, including changes in atmospheric transport. Improving the resolution of the data and analyzing ^{14}C in tree rings from other sites within the MCMA would help toward this.

The integration of the results presented here with the previous data obtained in the research program of ^{14}C dynamics in the MCMA are a step forward to understand the impact of different CO_2 emission sources in this complex urban area.

ACKNOWLEDGMENTS

This research was funded by DGAPA–UNAM (project PAPIIT-IN106113). Scholarships from CONACyT and Instituto de Geología for AMR are gratefully acknowledged. Thanks are also due to the authorities of Bosque de Chapultepec for granting permission for sampling the

tree-ring sequences. The authors gratefully acknowledge the NOAA Air Resources Laboratory (ARL) for the provision of the HYSPLIT transport and dispersion model and/or READY website (http://www.ready.noaa.gov) used in this publication. Comments by Jocelyn C Turnbull and an anonymous reviewer helped to improve this article.

REFERENCES

Beramendi-Orosco LE, Gonzalez-Hernandez G, Villanueva-Diaz J, Santos-Arevalo FJ, Gomez-Martinez I, Cienfuegos-Alvarado E, Morales-Puente P, Urrutia-Fucugauchi J. 2010. Modern radiocarbon levels for northwestern Mexico derived from tree rings—a comparison with Northern Hemisphere zones 2 and 3 curves. *Radiocarbon* 52(2–3):907–14.

Beramendi-Orosco LE, Sergio Hernandez-Morales S, Gonzalez-Hernandez G, Constante-Garcia V, Villanueva-Diaz J. 2013. Dendrochronological potential of *Fraxinus uhdei* and its use as bio-indicator of fossil CO_2 emissions deduced from radiocarbon concentrations in tree rings. *Radiocarbon* 55(3–4):833–40.

Beramendi-Orosco LE, Gonzalez-Hernandez G, Martinez-Jurado A, Martinez-Reyes A, Garcia-Samano A, Villanueva-Diaz J, Santos-Arevalo FJ, Gomez-Martinez I, Amador-Muñoz O. 2015. Temporal and spatial variations of atmospheric radiocarbon in the Mexico City Metropolitan Area. *Radiocarbon* 57(3):363–75.

Capano M, Marzaioli F, Sirignano C, Altieri S, Lubritto C, D'Onofrio A, Terrasi F. 2010. ^{14}C AMS measurements in tree rings to estimate local fossil CO_2 in Bosco Fontana forest (Mantova, Italy). *Nuclear Instruments and Methods in Physics Research B* 268:1113–16.

DDF (Departamento del Distrito Federal). 1990. Programa Integral contra la Contaminación Atmosférica (PICCA). Un compromiso común. Zona Metropolitana. México, D.F. Available at: http://www.aire.cdmx.gob.mx/descargas/publicaciones/flippingbook/picca/#p=1. Accessed October 2016.

DDF (Departamento del Distrito Federal). 1996. Programa para Mejorar la Calidad del Aire en el Valle de México (PROAIRE) 1995–2000. Available at: http://www.aire.cdmx.gob.mx/descargas/publicaciones/flippingbook/proaire1995-2000/. Accessed October 2016.

Djuricin S, Xu X, Pataki DE. 2012. The radiocarbon composition of tree rings as a tracer of local fossil fuel emissions in the Los Angeles basin: 1980–2008. *Journal of Geophysical Research* 117: D12302.

Doebelin EO. 1990. *Measurement Systems: Application and Design*. 4th edition. McGraw-Hill. 960 p.

Escamilla-Herrera I, Santos-Cerquera C. 2012. La Zona Metropolitana del Valle de México: transformación urbano-rural en la región Centro de México. In: XXII Coloquio Internacional de Geocrítica, Bogota, Colombia, 7–11 May 2012.

Graven HD, Gruber N. 2011. Continental-scale enrichment of atmospheric $^{14}CO_2$ from the nuclear power industry: potential impact on the estimation of fossil fuel-derived CO_2. *Atmospheric Chemistry and Physics* 11:12339–49.

Graven HD, Stephens BB, Guilderson TP, Campos TL, Schimel DS, Campbell JE, Keeling RF. 2009. Vertical profiles of biospheric and fossil fuel-derived CO_2 and fossil fuel CO_2:CO ratios from airborne measurements of $\Delta^{14}C$, CO_2 and CO above Colorado, USA. *Tellus* 61B:536–46.

Grootes PM, Farwell GW, Schmidt FH, Leach DD, Stuiver M. 1989. Rapid response of tree cellulose radiocarbon content to changes in atmospheric $^{14}CO_2$ concentration. *Tellus* 41B:134–48.

Harmon ME, Bond-Lamberty B, Tang J, Vargas R. 2011. Heterotrophic respiration in disturbed forests: a review with examples from North America. *Journal of Geophysical Research* 116:G00K04.

Hsueh DY, Krakauer NY, Randerson JT, Xu X, Trumbore SE, Southon JR. 2007. Regional patterns of radiocarbon and fossil fuel-derived CO_2 in surface air across North America. *Geophysical Research Letters* 34, L02816.

Hua Q, Barbetti M. 2004. Review of tropospheric bomb ^{14}C data for carbon cycle modeling and age calibration purposes. *Radiocarbon* 46(3):1273–98.

Hua Q, Barbetti M, Rakowski AZ. 2013. Atmospheric radiocarbon for the period 1950–2010. *Radiocarbon* 55(4):2059–72.

INEGI (Instituto Nacional de Estadística). 2014. Cuaderno estadístico y geográfico de la zona metropolitana del Valle de México. http://www.beta.inegi.org.mx/app/biblioteca/ficha.html?upc=702825068318. Accessed October 2016.

INEGI (Instituto Nacional de Estadística). 2016. Mapoteca Digital. http://cuentame.inegi.org.mx/mapas/nacional.aspx?tema=M. Accessed October 2016.

Jauregui E. 2004. Impact of land-use changes on the climate of the Mexico City Region. *Investigaciones Geográficas, Boletín del Instituto de Geografía, UNAM* 55:46–60.

Keller ED, Turnbull JC, Norris MW. 2016. Detecting long-term changes in point-source fossil CO_2 emissions with tree rings archives. *Atmospheric Chemistry and Physics* 16:5481–95.

Levin I, Kromer B, Schmidt M, Sartorius H. 2003. A novel approach for independent budgeting of fossil fuel CO_2 over Europe by $^{14}CO_2$ observations. *Geophysical Research Letters* 30(23):2194.

Levin I, Hammer S, Kromer B, Meinhardt F. 2008. Radiocarbon observations in atmospheric CO_2:

determining fossil fuel CO_2 over Europe using Jungfraujoch observations as background. *Science of the Total Environment* 391:211–6.

Levin I, Rödenbeck C. 2008. Can the envisaged reductions of fossil fuel CO_2 emissions be detected by atmospheric observations? *Naturwissenschaften* 95:203–8.

Nemec M, Wacker L, Hajdas I, Gäggeler H. 2010. Alternative methods for cellulose preparation for AMS measurement. *Radiocarbon* 52(2–3): 1358–70.

OECD (Organisation for Economic Co-operation and Development). 2013. OECD Environmental Performance Reviews: Mexico 2013, OECD Publishing. Available at: http://www.oecd.org/mexico/oecd-environmental-performance-reviews-mexico-2013-9789264180109-en.htm. Accessed October 2016.

Rakowski AZ, Pawelczyk S, Pazdur A. 2001. Changes of ^{14}C concentration in modern trees from Upper Silesia region, Poland. *Radiocarbon* 43 (2B): 679–89.

Rakowski AZ, Nakamura T, Pazdur A. 2008. Variations of anthropogenic CO_2 in urban area deduced by radiocarbon concentration in modern tree rings. *Journal of Environmental Radioactivity* 99(10):1558–65.

Randerson JT, Enting IG, Schuur EAG, Caldeira K, Fung IY. 2002. Seasonal and latitudinal variability of troposphere $D^{14}CO_2$: post bomb contributions from fossil fuels, oceans, the stratosphere, and the terrestrial biosphere. *Global Biogeochemical Cycles* 16(4):1112.

Reimer PJ, Brown TA, Reimer RW. 2004. Discussion: reporting and calibration of post-bomb ^{14}C data. *Radiocarbon* 46(3):1299–304.

Rolph G, Stein A, Stunder B. 2017. Real-time Environmental Applications and Display sYstem: READY. *Environmental Modelling & Software* 95:210–28.

SEDEMA (Secretaría del Medio Ambiente de la Ciudad de México). 2000. Inventario de emisiones a la atmósfera Zona Metropolitana del Valle de México 2000. Available at: http://www.aire.cdmx.gob.mx/descargas/publicaciones/flippingbook/inventario-emisiones-zmvm2000/#p=1. Accessed October 2016.

SEDEMA (Secretaría del Medio Ambiente de la Ciudad de México). 2012. Inventario de emisiones contaminantes y de efecto invernadero de la Zona Metropolitana del Valle de México 2010. Available at: http://www.aire.cdmx.gob.mx/descargas/publicaciones/flippingbook/inventario-emisiones-zmvm-gei2010/. Accessed October 2016.

SEDEMA (Secretaría del Medio Ambiente de la Ciudad de México). 2016. Inventario de Emisiones de la CDMX 2014, contaminantes criterio, tóxicos y de efecto invernadero. Avalilable at: http://www.aire.cdmx.gob.mx/descargas/publicaciones/flippingbook/inventario-emisiones-cdmx2014-2/. Accessed October 2016.

Stahle DW, Villanueva-Diaz J, Burnette DJ, Cerano-Paredes J, Heim RR, Fye FK, Acuña-Soto R, Therrell MD, Cleaveland MK, Stahle DK. 2011. Major Mesoamerican droughts of the past millennium. *Geophysical Research Letters* 38(5):L05703.

Stein AF, Draxler RR, Rolph GD, Stunder BJB, Cohen MD, Ngan F. 2015. NOAA's HYSPLIT atmospheric transport and dispersion modeling system. *Bulletin of the American Meteorological Society* 96:2059–77.

Stokes MA, Smiley TL. 1968. *An Introduction to Tree-Ring Dating*. Chicago: University of Chicago Press. 73 p.

Stuiver M, Polach HA. 1977. Discussion: reporting of ^{14}C data. *Radiocarbon* 19(3):355–63.

Synal HA, Stocker M, Suter M. 2007. MICADAS: a new compact radiocarbon AMS system. *Nuclear Instruments and Methods B* 259(1):7–13.

Tans P, Keeling R. 2016. Trends in Atmospheric Carbon Dioxide, Mauna Loa CO_2 annual mean data. Available at: ftp://aftp.cmdl.noaa.gov/products/trends/co2/co2_annmean_mlo.txt. Accessed October 2016.

Turnbull JC, Miller JB, Lehman SJ, Tans PP, Sparks RJ, Southon J. 2006. Comparison of $^{14}CO_2$, CO, and SF_6 as tracers for recently added fossil fuel CO_2 in the atmosphere and implications for biological CO_2 exchange. *Geophysical Research Letters* 33:L01817.

Turnbull JC, Sweeney C, Karion A, Newberger T, Lehman SJ, Tans PP, Davis KJ, Lauvaux T, Miles NL, Richardson SJ, Cambaliza MO, Shepson PB, Gurney K, Patarasuk R, Razlivanov I. 2015. Toward quantification and source sector identification of fossil fuel CO_2 emissions from an urban area: Results from the INFLUX experiment. *Journal of Geophysical Research Atmospheres* 120:292–312.

Turnbull JC, Graven HD, Krakauer NY. 2016. Radiocarbon in the atmosphere. In: Schuur EAG, Druffel ERM, Trumbore SE, editors. *Radiocarbon and Climate Change*. Springer International Publishing. p 83–137.

Vay SA, Tyler SC, Choi Y, Blake DR, Blake NJ, Sachse GW, Diskin GS, Singh HB. 2009. Sources and transport of $\Delta^{14}C$ in CO_2 within the Mexico City Basin and vicinity. *Atmospheric Chemistry and Physics* 9:4973–85.

Villanueva-Díaz J, Stahle DW, Therrel MD, Cleaveland MK, Camacho Morfín F, Núñez Díaz de la Fuente P, Gómez Chávez S, Sánchez Sesma J, Ramírez García JA. 2003. Registros climáticos de los ahuehuetes de Chapultepec en los últimos 450 años. *Boletín del Archivo Histórico del Agua* 23:34–43.

Wacker L, Nemeç M, Bourquin J. 2010a. A revolutionary graphitisation system: fully automated, compact and simple. *Nuclear Instruments and Methods in Physics Research B* 268(7–8):931–4.

Wacker L, Christl M, Synal H-A. 2010b. Bats: a new tool for AMS data reduction. *Nuclear Instruments and Methods in Physics Research B* 268(7–8): 976–9.

https://doi.org/10.1017/RDC.2017.100 Published online by Cambridge University Press